

Thermodynamic properties of two-dimensional charged spin-1/2 Fermi gases

Jia-Ying Yang(杨家营), Xu Liu(刘旭), Ji-Hong Qin(秦吉红), and Huai-Ming Guo(郭怀明)

Citation: Chin. Phys. B, 2022, 31 (**6**): 060504. DOI: 10.1088/1674-1056/ac4e0b
Journal homepage: http://cpb.iphy.ac.cn; http://iopscience.iop.org/cpb

What follows is a list of articles you may be interested in

The dynamics of a memristor-based Rulkov neuron with fractional-order difference

Yan-Mei Lu(卢艳梅), Chun-Hua Wang(王春华), Quan-Li Deng(邓全利), and Cong Xu(徐聪)
Chin. Phys. B, 2022, 31 (**6**): 060502. DOI: 10.1088/1674-1056/ac539a

Complex dynamic behaviors in hyperbolic-type memristor-based cellular neural network

Ai-Xue Qi(齐爱学), Bin-Da Zhu(朱斌达), and Guang-Yi Wang(王光义)
Chin. Phys. B, 2022, 31 (**2**): 020502. DOI: 10.1088/1674-1056/ac2b1b

Three-dimensional spin–orbit coupled Fermi gases: Fulde–Ferrell pairing, Majorana fermions, Weyl fermions, and gapless topological superfluidity

Xia-Ji Liu, Hui Hu, Han Pu
Chin. Phys. B, 2015, 24 (**5**): 050502. DOI: 10.1088/1674-1056/24/5/050502

The stability of a non-extensive relativistic Fermi system

Wang Hai-Tang, Men Fu-Dian, He Xiao-Gang, Wei Qun-Mei
Chin. Phys. B, 2012, 21 (**6**): 060501. DOI: 10.1088/1674-1056/21/6/060501

Oscillating Casimir force between two slabs in a Fermi sea

Chen Li-Wei, Su Guo-Zhen, Chen Jin-Can, Andresen Bjarne
Chin. Phys. B, 2012, 21 (**1**): 010501. DOI: 10.1088/1674-1056/21/1/010501

Thermodynamic properties of two-dimensional charged spin-1/2 Fermi gases

Jia-Ying Yang(杨家营)[1], Xu Liu(刘旭)[1], Ji-Hong Qin(秦吉红)[1,2,†], and Huai-Ming Guo(郭怀明)[3]

[1] *Department of Physics, University of Science and Technology Beijing, Beijing* 100083, *China*
[2] *Institute of Theoretical Physics, University of Science and Technology Beijing, Beijing* 100083, *China*
[3] *Department of Physics, Beihang University, Beijing* 100191, *China*

(Received 28 December 2021; accepted manuscript online 24 January 2022)

Based on the mean-field theory, we investigate the thermodynamic properties of the two-dimensional (2D) charged spin-1/2 Fermi gas. Landé factor g is introduced to measure the strength of the paramagnetic effect. There is a competition between diamagnetism and paramagnetism in the system. The larger the Landé factor, the smaller the entropy and specific heat. Diamagnetism tends to increase the entropy, while paramagnetism leads to the decrease of the entropy. We find that there exists a critical value of Landé factor for the transition point due to the competition. The entropy of the system increases with the magnetic field when $g < 0.58$. With the growth of paramagnetism, when $g > 0.58$, the entropy first decreases with the magnetic field, then reaches a minimum value, and finally increases again. Both the entropy and specific heat increase with the temperature, and no phase transition occurs. The specific heat tends to a constant value at the high-temperature limit, and it approaches to zero at very low temperatures, which have been proved by the analytical calculation.

Keywords: Fermi gas, entropy, specific heat, Landé factor

PACS: 05.30.–d, 05.30.Fk, 75.20.–g **DOI:** 10.1088/1674-1056/ac4e0b

1. Introduction

With the realization of many important results of ultracold atomic Fermi systems,[1–7] the study of Fermi systems has attracted a great deal of interest and becomes an active and rich field. Although the Fermi gases cannot occur Bose–Einstein condensation like Bose gases at low temperatures, the low-temperature behavior of the Fermi gas system is also worthy of note. Under appropriate conditions, fermions can form Cooper pairs and thus have the macroscopic quantum effects of Bose system, such as superconductivity and superfluidity.[8,9] The properties of the Fermi gas are influenced by a variety of factors, including the total number of particles in the system, the spatial dimension, the energy spectrum dispersion relation and the interaction between all Fermi gas particles. Previous studies have introduced a number of approximate methods to study the affected factors of the systems specifically. For example, the first order energy level of the Fermi system with hard-sphere interaction is calculated using pseudopotential method.[10] The thermodynamic properties of ideal Fermi gases in a harmonic potential are studied under the generalized uncertainty principle applying Thomas–Fermi approximation.[11] Furthermore, the free energy applied to various problems in statistical mechanics is also investigated based on variational principle of Bogoliubov.[12]

In the study of quantum systems, using external potential to restrict is also an important research method.[13,14] The statistical properties have been investigated for the nonrelativistic charged spinless bosons in constant magnetic field.[15] However, for further study of statistical properties of quantum gases, it is necessary to consider both orbital and spin degrees of freedom. The analytical result of thermodynamic potential of the weakly interaction Fermi gas has been calculated on the bases of considering the orbital motion and spin motion of particles. It has been found that using the magnetic field always causes energy and stability decrease and chemical potential increase of the system.[16] In our previous work, we have investigated the magnetic properties of charged spin Bose and Fermi gases with ferromagnetic coupling.[17,18] They are helpful to further exploration of macroscopic quantum phenomena in the system of cold atoms.

Since 2D quantum systems can exhibit behaviors which are not found in three dimensions,[19,20] low-dimensional configurations of Fermi gases have also become the subject of theoretical and experimental studies.[21,22] Researches on 2D Fermi systems contribute to the understanding of important frontier scientific problems such as unconventional superconductors,[23] graphene,[24] topological insulator materials[25] as well as Majorana mode.[26] On the theoretical side, the evolution from a superfluid state with large Cooper pairs to a superfluid state with compact molecules has been studied in the 2D attracting fermion system.[27] Recently, the thermodynamic quantities as functions of temperature, interaction strength and effective range,[28] and the role of a negative confinement-induced effective range on many-body pairing above the superfluid transition[29] in the strongly correlated 2D Fermi gases are also in-

†Corresponding author. E-mail: jhqin@sas.ustb.edu.cn

© 2022 Chinese Physical Society and IOP Publishing Ltd

vestigated. Experimentally, 2D Fermi gases have been solved their production,[30–32] pairing,[33,34] pseudogap,[35] pressure profiles,[36] the Berezinskii–Kosterlitz–Thouless transition,[37] etc. The study of 2D Fermi gases provides an important tool for understanding confined many-body systems in physics.

In this paper, we will focus on the entropy and specific heat of the 2D charged spin-1/2 Fermi gas. Under the mean-field approximation, the orbital motion and spin motion of particles are considered simultaneously. The Landé factor g is introduced to measure the strength of paramagnetism. The effect of temperature, Landé factor and magnetic field on the entropy and specific heat are investigated. The remainder of this paper is organized as follows. Section 2 introduces a model consisting of Landau diamagnetism and Pauli paramagnetism. The entropy, specific heat as well as the magnetization density are calculated respectively. Section 3 presents the result of detailed analysis and discussion. Section 4 concludes this article.

2. Theoretical model

We consider the orbital motion of 2D charged Fermi gas of N particles with mass m^* in a constant magnetic field B in the z-direction. The quantized Landau energy level is

$$\varepsilon_j^l = \left(j+\frac{1}{2}\right)\hbar\omega, \tag{1}$$

where $j = 0,\ 1,\ 2,\ \ldots$ labels the different Landau levels and $\omega = qB/(m^*c)$ is the gyromagnetic frequency. ω can be used to indicate the strength of the magnetic field according to $\omega \propto B$. The energy levels in the x–y plane are degenerate with degeneracy

$$D_{\rm L} = \frac{qBA}{2\pi\hbar c}, \tag{2}$$

where A is the section area of x–y in the system.

For a spin $-1/2$ fermion, the intrinsic magnetic moment in a magnetic field results in Zeeman splitting, the energy level can be written as

$$\varepsilon_\sigma^{\rm ze} = -g\sigma\frac{q\hbar}{m^*c}B = -g\sigma\hbar\omega, \tag{3}$$

where g refers to the Landé factor and σ is the spin-z index of Zeeman state $|F=1, m_F=\sigma\rangle\,(\sigma=+1/2,-1/2)$. The Zeeman effect causes the Pauli paramagnetism and the quantization of the orbital motion leads to the Landau diamagnetism.

The effective Hamiltonian of the system of N fermions can be expressed by the following equation:

$$\bar{H}-\mu N = D_{\rm L}\sum_{j,\sigma}\left(\varepsilon_j^l+\varepsilon_\sigma^{\rm ze}-\mu\right)n_{j\sigma}, \tag{4}$$

where μ is the chemical potential, and the effective Hamiltonian of the system can be used to derive the grand thermodynamic potential

$$\begin{aligned}\Omega_{T\neq0} &= -\frac{1}{\beta}\ln{\rm Tr}\,{\rm e}^{-\beta(\bar{H}-\mu N)}\\ &= -\frac{m^*\omega A}{2\pi\beta\hbar}\sum_{j,\sigma}\ln\{1+{\rm e}^{-\beta\left[\left(\frac{1}{2}+j\right)\hbar\omega-g\sigma\hbar\omega-\mu\right]}\},\end{aligned} \tag{5}$$

where $\beta = (k_{\rm B}T)^{-1}$. By conducting a Taylor expansion and then combining the terms of the series containing j, we have

$$\Omega_{T\neq0} = -\frac{m^*\omega A}{2\pi\beta\hbar}\sum_{l=1}^{\infty}\sum_{\sigma}\frac{(-1)^{l+1}l^{-1}\,{\rm e}^{-l\beta\left[\frac{\hbar\omega}{2}-g\sigma\hbar\omega-\mu\right]}}{1-{\rm e}^{-l\beta\hbar\omega}}. \tag{6}$$

We introduce the following notation for sum simplicity:

$$F_\tau^\sigma[\alpha,\delta] = \sum_{l=1}^{\infty}\frac{(-1)^{l+1}l^{\alpha/2}\,{\rm e}^{-l\beta\left(\frac{1}{2}\hbar\omega-g\sigma\hbar\omega-\mu+\delta\right)}}{\left(1-{\rm e}^{-l\beta\hbar\omega}\right)^\tau}, \tag{7}$$

then Eq. (6) can be rewritten as

$$\Omega_{T\neq0} = -\frac{m^*\omega A}{2\pi\beta\hbar}\sum_{\sigma}F_1^\sigma\left[-2,0\right]. \tag{8}$$

The density of particles $n = N/A$ of the system is given by the grand thermodynamic potential

$$n_{T\neq0} = -\frac{1}{A}\left(\frac{\partial\Omega_{T\neq0}}{\partial\mu}\right)_{T,A} = \frac{m^*\omega}{2\pi\hbar}\sum_{\sigma}F_1^\sigma\left[0,0\right]. \tag{9}$$

In the grand canonical ensemble, we can get the expression of entropy

$$\begin{aligned}S &= k_{\rm B}\beta^2\left(\frac{\partial\Omega_{T\neq0}}{\partial\beta}\right)_{\mu,A}\\ &= k_{\rm B}\frac{m^*\omega A}{2\pi\hbar}\left\{\sum_{\sigma}F_1^\sigma[-2,0]+x\sum_{\sigma}F_2^\sigma[0,1]\right.\\ &\quad\left.+\sum_{\sigma}\beta\left(\frac{1}{2}\hbar\omega-g\sigma\hbar\omega-\mu\right)F_1^\sigma[0,0]\right\},\end{aligned} \tag{10}$$

where $x = \beta\hbar\omega$. The magnetization density can be derived as

$$\begin{aligned}M_{T\neq0} &= -\frac{1}{A}\left(\frac{\partial\Omega_{T\neq0}}{\partial B}\right)_{T,A}\\ &= \frac{q}{2\pi\hbar\beta c}\left\{\sum_{\sigma}F_1^\sigma[-2,0]-x\sum_{\sigma}F_2^\sigma[0,1]\right.\\ &\quad\left.-x\sum_{\sigma}\left(\frac{1}{2}-g\sigma\right)F_1^\sigma[0,0]\right\}.\end{aligned} \tag{11}$$

Furthermore, we can obtain the internal energy U through grand thermodynamic potential $\Omega_{T\neq0}$ of the system

$$\begin{aligned}U &= \frac{\partial}{\partial\beta}\left(\beta\Omega_{T\neq0}\right)\\ &= \frac{m^*\omega^2A}{2\pi}\left\{\sum_{\sigma}F_2^\sigma[0,1]+\sum_{\sigma}\left(\frac{1}{2}-g\sigma\right)F_1^\sigma[0,0]\right\},\end{aligned} \tag{12}$$

the specific heat of the system can be obtained as

$$C_V = -k_{\rm B}\beta^2\left(\frac{\partial U}{\partial\beta}\right)_A$$

$$= k_{\rm B}\beta\frac{m^*\omega^2 A}{2\pi}\left\{x\sum_\sigma F_2^\sigma[2,1]+2x\sum_\sigma F_3^\sigma[2,2] +x\left(\eta_\sigma+\beta\frac{\partial}{\partial\beta}\eta_\sigma\right)\sum_\sigma F_2^\sigma[2,1]\right\}, \tag{13}$$

where $\eta_\sigma=\frac{1}{2}-g\sigma-\frac{\mu}{\hbar\omega}$. Through the conservation of particle number density, we can derive

$$x\left(\eta_\sigma+\beta\frac{\partial}{\partial\beta}\eta_\sigma\right)=-\frac{x\sum_\sigma F_2^\sigma[2,1]}{\sum_\sigma F_1^\sigma[2,0]}. \tag{14}$$

Substituting Eq. (14) into Eq. (13), we get

$$C_V = k_{\rm B}\left(\frac{m^*\omega A}{2\pi\hbar}\right)x^2\sum_\sigma\left\{F_2^\sigma[2,1]+2F_3^\sigma[2,2] -\frac{(F_2^\sigma[2,1])^2}{F_1^\sigma[2,0]}\right\}. \tag{15}$$

For simplicity of calculation, we introduce the following dimensionless parameters: $\bar{\omega}=\hbar\omega/(k_{\rm B}T^*)$, $t=T/T^*$, $\bar{\mu}=\mu/(k_{\rm B}T^*)$, $\bar{S}=S/(Nk_{\rm B})$, $\bar{M}_{T\neq0}=m^*cM/(n\hbar q)$, $\bar{C}_V=C_V/(Nk_{\rm B})$, then $x=\bar{\omega}/t$, T^* is the characteristic temperature given by $k_{\rm B}T^*=2\pi\hbar^2n/m^*$.

After the process of dimensionless, Eqs. (9)–(11) and (15) can be re-expressed respectively as

$$1 = \bar{\omega}\sum_\sigma\bar{F}_1^\sigma[0,0], \tag{16}$$

$$\bar{S} = xt\sum_\sigma\bar{F}_1^\sigma[-2,0]+x^2t\sum_\sigma\bar{F}_2^\sigma[0,1] +x\left(\frac{1}{2}\bar{\omega}-g\sigma\bar{\omega}-\bar{\mu}\right)\sum_\sigma\bar{F}_1^\sigma[0,0], \tag{17}$$

$$\bar{M}_{T\neq0} = t\sum_\sigma\bar{F}_1^\sigma[-2,0]-x\sum_\sigma\bar{F}_2^\sigma[0,1] -x\left(\frac{1}{2}-g\sigma\right)\sum_\sigma\bar{F}_1^\sigma[0,0], \tag{18}$$

$$\bar{C}_V = x^3t\left\{\sum_\sigma\bar{F}_2^\sigma[2,1]+2\sum_\sigma\bar{F}_3^\sigma[2,2] -\frac{(\sum_\sigma\bar{F}_2^\sigma[2,1])^2}{\sum_\sigma\bar{F}_1^\sigma[2,0]}\right\}, \tag{19}$$

where

$$\bar{F}_\tau^\sigma[\alpha,\delta]=\sum_{l=1}^{\infty}\frac{(-1)^{l+1}l^{\alpha/2}\,{\rm e}^{-lx(\frac{1}{2}-g\sigma-\frac{\bar{\mu}}{\bar{\omega}}+\delta)}}{(1-{\rm e}^{-lx})^\tau}, \tag{20}$$

and $\bar{\mu}$ is the dimensionless parameter of the chemical potential, which can be determined from the mean-field self-consistent Eq. (16).

3. Results and discussion

The evolution of entropy and specific heat with the inverse of temperature of the 2D charged spin-1/2 Fermi gas in the external magnetic field is plotted in Fig. 1. It can be seen that both the entropy and specific heat decrease monotonically with the increases of the inverse of temperature, which means that there is no phase transition. At low temperature, both the entropy and specific heat tend to a constant for different magnetic fields and the specific heat approaches to zero. On the other hand, it can be seen that the curve of entropy as well as the specific heat at different magnetic fields tends to overlap when the temperature is high, and the specific heat reaches a constant value 1. It shows that the magnetic field has little effect on the entropy and specific heat under the high-temperature limit.

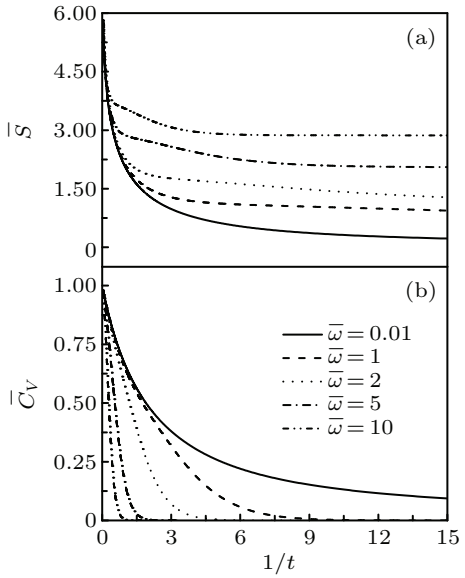


Fig. 1. The entropy $\bar{S}$ and specific heat $\bar{C}_V$ as the function of $1/t$ for fixed Landé factor $g=0.1$, the value of $\bar{\omega}$ are in sequence as $\bar{\omega}=0.01$ (solid line), 1 (dashed line), 2 (dotted line), 5 (dash dotted line), 10 (dash dot dotted line).

Furthermore, to reconfirm our numerical results, we derive the analytical expressions in the limit case. Under the high-temperature limit, the Fermi–Dirac statistics reduce to Boltzmann statistics, the grand thermodynamic potential of the system can be rewritten as

$$\Omega^B_{T\neq0} = -\frac{1}{\beta}D_l\sum_{j,\sigma}{\rm e}^{-\beta(\varepsilon_j^l+\varepsilon_\sigma^{ze}-\mu)} = -\frac{m^*\omega A}{2\pi\beta\hbar}\sum_\sigma\frac{{\rm e}^{-\beta\left(\frac{1}{2}\hbar\omega-g\sigma\hbar\omega-\mu\right)}}{1-{\rm e}^{-\beta\hbar\omega}}. \tag{21}$$

Then the expression of the self-consistent equation in this system can be derived as follows:

$$1=\bar{\omega}\sum_\sigma\frac{{\rm e}^{-x\left(\frac{1}{2}-g\sigma-\frac{\bar{\mu}}{\bar{\omega}}\right)}}{1-{\rm e}^{-x}}. \tag{22}$$

Substituting Eq. (22) into Eq. (19), the analytical expression of the specific heat can be obtained as

$$\bar{C}_V^B=x^2\left\{-\left(\frac{{\rm e}^{-x}}{1-{\rm e}^{-x}}\right)^2+\frac{{\rm e}^{-x}}{1-{\rm e}^{-x}}+\frac{2{\rm e}^{-2x}}{(1-{\rm e}^{-x})^2}\right\}. \tag{23}$$

The limit value of $\bar{C}_V^B$ can be obtained exactly by Eq. (23) $\bar{C}_V^B|_{x\to0}=1$ and $\bar{C}_V^B|_{x\to\infty}=0$. Thus, our numerical results

correspond very well to the conclusions of the analytical derivation at high and low temperature limits.

To show the effect of paramagnetism, we plot the evolution of the entropy and specific heat with Landé factor g under different magnetic fields in Fig. 2. As can be seen from Fig. 2(a), the entropy decreases with the increase of Landé factor, indicating that paramagnetism can reduce the entropy of the system. An intersection point is shown in the figure. On the left side of the intersection point, the entropy increases with the increase of the magnetic field, while on the right side of the intersection point, the entropy decreases with the increase of the magnetic field. The existence of intersection point indicates that there is a critical value of Landé factor g. When the Landé factor is less than this critical value, diamagnetism leads to the increase of entropy, but when the Landé factor is greater than this critical value, the effect of paramagnetism on the decrease of entropy is greater than that of diamagnetism on the increase of entropy. It can also be found that the intersection point is basically unchanged under different magnetic fields in this range. As shown in Fig. 2(b), paramagnetism can cause the decrease of the specific heat. Furthermore, when the Landé factor g is constant, the specific heat decreases with the increase of the magnetic field, indicating that the enhancement of the magnetic field can reduce the specific heat of the system. When the magnetic field is small, the variation of the entropy and specific heat as the function of Landé factor g is very small, which suggests that the paramagnetism has little effect on the entropy and specific heat of the system under the weak magnetic field.

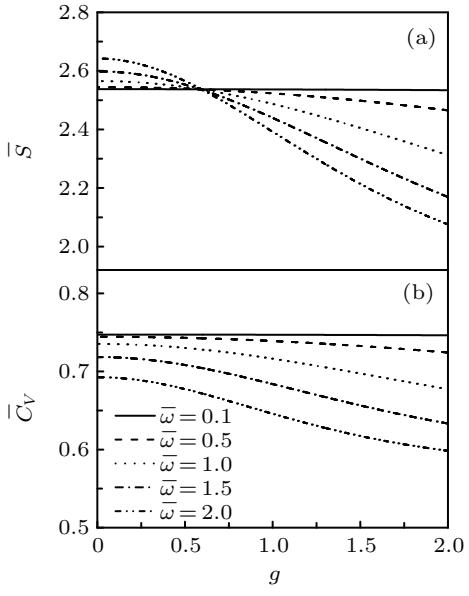


Fig. 2. The entropy $\bar{S}$ and specific heat $\bar{C}_V$ as a function of g at $t = 1.5$ for different magnetic field $\bar{\omega} = 0.1$ (solid line), 0.5 (dashed line), 1 (dotted line), 1.5 (dash dotted line), 2 (dash dot dotted line).

In order to explain Fig. 2(a) more clearly, it is necessary to find the critical Landé factor g_c to describe the competition between the paramagnetism and diamagnetism when $\bar{M}_{T\neq 0} = 0$. Figure 3 plots g_c as the function of $\bar{\omega}$. Obviously, g_c decreases monotonically with decreasing magnetic field, and $g_c|_{\bar{\omega}\to 0} \approx 0.58$ for different temperatures. Although the exact value of g_c in the very high magnetic field can not obtained, we can estimate that the value of g_c ranges from 0.58 to 1. The illustration in Fig. 3 shows that g_c changes little with the magnetic field in the low magnetic field, which can explain why the intersection point of Fig. 2(a) is basically not affected by the magnetic field.

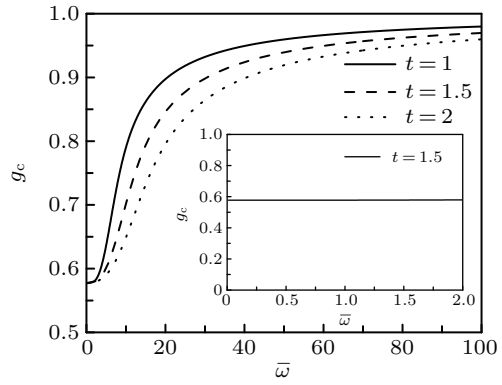


Fig. 3. The critical value of Landé factor g_c as the function of $\bar{\omega}$ for fixed value of t, the temperature t is chosen as $t = 1$ (solid line), 1.5 (dashed line), 2 (dotted line). The inset depicts the relationship of g_c versus magnetic field $\bar{\omega}$, and the temperature $t = 1.5$.

In addition, we also calculate the analytical results of g_c in the weak and strong magnetic field limits. The expression of $\bar{M}^B_{T\neq 0}$ can be derived by Eq. (21)

$$\bar{M}^B_{T\neq 0} = t\sum_{\sigma}\left\{\frac{\mathrm{e}^{-\frac{1}{t}\left(\frac{1}{2}\bar{\omega}-g\sigma\bar{\omega}-\bar{\mu}\right)}}{1-\mathrm{e}^{-x}} \times\left[1+x\left(g\sigma-\frac{1}{2}-\frac{\mathrm{e}^{-x}}{1-\mathrm{e}^{-x}}\right)\right]\right\}. \tag{24}$$

Substituting Eq. (22) into Eq. (24), we obtain

$$\bar{M}^B_{T\neq 0} = \frac{1}{x}-\frac{1}{2}-\frac{1}{\mathrm{e}^x-1}+\frac{g\left(\mathrm{e}^{gx}-1\right)}{2\left(\mathrm{e}^{gx}+1\right)}, \tag{25}$$

where $x = \bar{\omega}/t$. As $\bar{M}^B_{T\neq 0} = 0$, the limit value of g_c can be derived: $g_c|_{\bar{\omega}\to 0} = 1/\sqrt{3} \approx 0.577$ and $g_c|_{\bar{\omega}\to\infty} = 1$. The numerical results in Fig. 3 are consistent with the analytical derivation. Therefore, it is reasonable for the system always exhibits diamagnetism when $g_c < 0.577$. And a transition from diamagnetism to paramagnetism will occur when $0.577 < g_c < 1$.

Since the magnetic field is an important factor affecting entropy and specific heat, we plot Fig. 4 to focus on the effect of magnetic field. As shown in Fig. 4(a), when the Landé factor is small, the entropy increases with the increase of the magnetic field. With the increase of the Landé factor, the entropy first decreases with the increase of the magnetic field, reaches a minimum value, and then increases with the increase of the magnetic field. $g_c = 0.58$ is the critical value for this transition. When g is less than the critical value, diamagnetism is stronger than paramagnetism, so the entropy increases with the increase of the magnetic field. However, with the increase of g,

paramagnetism gradually prevails. When g is greater than the critical value, the paramagnetism exceeds the diamagnetism. When paramagnetism is dominant, the entropy first decreases with the increase of the magnetic field. With the increase of the magnetic field, diamagnetism overcomes paramagnetism after entropy reaches the lowest point, and the entropy begins to rise with the increase of the magnetic field. The illustration shows in detail the evolution of entropy with magnetic field near the critical value of Landé factor. $g = 0.5$ is below the critical value. It is obvious that the entropy increases monotonically with the magnetic field. While $g = 0.7$ is above the critical value. The entropy initially shows a downward trend with the magnetic field at low magnetic field. Then we discuss the specific heat in Fig. 4(b). The specific heat decreases with the increase of the magnetic field, which coincides with Fig. 2(b). When the Landé factor is larger than 0.58, the specific heat still decreases with the increase of the magnetic field, but the magnitude of the decrease becomes large. It shows that the reduction of specific heat is enhanced after paramagnetism is dominant. It also finds that the larger the Landé factor, the smaller the values of entropy and specific heat for a constant magnetic field. This is consistent with the conclusion we obtained in Fig. 2 that both the entropy and specific heat decrease with the growth of paramagnetism.

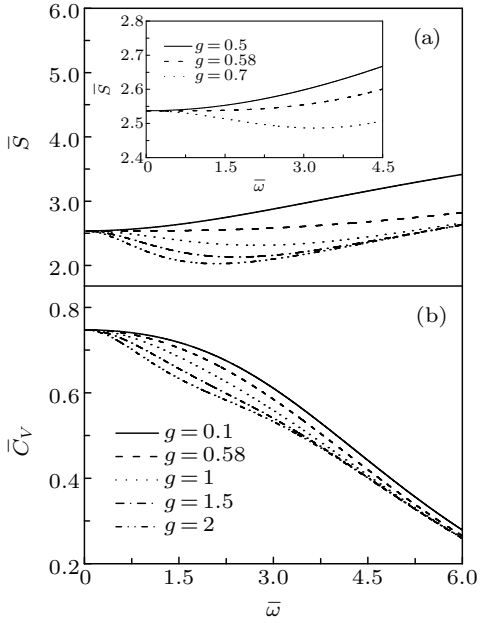


Fig. 4. The entropy $\bar{S}$ and specific heat $\bar{C}_V$ as a function of $\bar{\omega}$ for $t = 1.5$. The Landé factor g is taken as $g = 0.1$ (solid line), 0.58 (dashed line), 1 (dotted line), 1.5 (dash dotted line), 2 (dash dot dotted line), respectively. The inset depicts the relationship of $\bar{S}$ versus magnetic field $\bar{\omega}$ with the magnetic field region lies between 0 and 4.5, and the Landé factor g is chosen as $g = 0.5$ (solid line), 0.58 (dashed line), 0.7 (dotted line).

4. Conclusion

This paper discusses the variation of the entropy and specific heat of the 2D charged spin-1/2 Fermi gas with respect to the inverse of temperature $1/t$, Landé factor g, and the magnetic field $\bar{\omega}$. Our results show that both the entropy and specific heat decrease with the increase of the Landé factor. It is indicated that the increase of paramagnetism can decrease the entropy and specific heat. The effect of paramagnetism on the entropy and specific heat is relatively small when the magnetic field is weak. The specific heat decreases with the magnetic field and eventually approaches zero. There is a competition between the diamagnetism and paramagnetism in the system. The system always exhibits diamagnetism and entropy increases with magnetic field when $g_c < 0.58$. However, when $g_c > 0.58$, paramagnetism is gradually enhanced. The entropy first decreases with the increase of the magnetic field, and then increases after a minimum value. Furthermore, the specific heat increases monotonically with the temperature and ultimately reaches a constant value. Here no phase transition point appears. Our result shows that there is no spontaneous breaking of continuous symmetries in this system.

Acknowledgements

Project supported by the National Natural Science Foundation of China (Grant No. 11774019) and the Fundamental Research Funds for the Central Universities, China (Grant No. FRF-BR-16-014A).

References

[1] Regal C A, Ticknor C, Bohn J L and Jin D S 2003 *Nature* **424** 47
[2] Xiong H W, Liu S J, Zhang W P and Zhan M S 2005 *Phys. Rev. Lett.* **95** 120401
[3] Qin F and Chen J S 2009 *Phys. Rev. A* **79** 043625
[4] Chen J S, Cheng C M, Li J R and Wang Y P 2007 *Phys. Rev. A* **76** 033617
[5] Kinast J, Hemmer S L, Gehm M E, Turlapov A and Thomas J E 2004 *Phys. Rev. Lett.* **92** 150402
[6] Bartenstein M, Altmeyer A, Riedl S, Jochim S, Chin C, Denschlag J H and Grimm R 2004 *Phys. Rev. Lett.* **92** 203201
[7] Kinast J, Turlapov A, Thomas J E, Chen Q J, Stajic J and Levin K 2005 *Science* **307** 1296
[8] Bardeen J, Cooper L N and Schrieffer J R 1957 *Phys. Rev.* **108** 1175
[9] Zwierlein M W, Abo-Shaeer J R, Schirotzek A, Schunck C H and Ketterle W 2005 *Nature* **435** 1047
[10] Huang K and Yang C N 1957 *Phys. Rev.* **105** 767
[11] Li H L, Ren J X, Wang W W, Yang B and Shen H J 2018 *J. Stat. Mech.: Theory Exp.* **2018** 023106
[12] Kuzemsky A L 2015 *Int. J. Mod. Phys. B* **29** 1530010
[13] Regal C A, Greiner M and Jin D S 2004 *Phys. Rev. Lett.* **92** 040403
[14] Jochim S, Bartenstein M, Altmeyer A, Hendl G, Riedl S, Chin C, Denschlag J H and Grimm R 2003 *Science* **302** 2101
[15] Standen G B and Toms D J 1999 *Phys. Rev. E* **60** 5275
[16] Men F D, Liu H and Zhu H Y 2008 *Sci. China Ser. G* **51** 1072
[17] Qin J H, Jian X L and Gu Q 2012 *J. Phys.: Condensed. Matter* **24** 366007
[18] Wang B B, Qin J H and Guo H M 2015 *Eur. Phys. J. B* **88** 246
[19] Mermin N D and Wagner H 1966 *Phys. Rev. Lett.* **17** 1133
[20] Hohenberg P C 1967 *Phys. Rev.* **158** 383
[21] Giorgini S, Pitaevskii L P and Stringari S 2008 *Rev. Mod. Phys.* **80** 1215
[22] Bloch I, Dalibard J and Zwerger W 2008 *Rev. Mod. Phys.* **80** 885
[23] Dagotto E 1994 *Rev. Mod. Phys.* **66** 763
[24] Geim A K and Novoselov K S 2007 *Nat. Mater.* **6** 183
[25] Hasan M Z and Kane C L 2010 *Rev. Mod. Phys.* **82** 3045

[26] Xu J P, Wang M X, Liu Z L, Ge J F, Yang X J, Liu C H, Xu Z A, Guan D D, Gao C L, Qian D, Liu Y, Wang Q H, Zhang F C, Xue Q K and Jia J F 2015 *Phys. Rev. Lett.* **114** 017001
[27] Randeria M, Duan J M and Shieh L Y 1989 *Phys. Rev. Lett.* **62** 981
[28] Mulkerin B C, Hu H and Liu X J 2020 *Phys. Rev. A* **101** 013605
[29] Mulkerin B C, Liu X J and Hu H 2020 *Phys. Rev. A* **102** 013313
[30] Modugno G, Ferlaino F, Heidemann R, Roati G and Inguscio M 2003 *Phys. Rev. A* **68** 011601
[31] Martiyanov K, Makhalov V and Turlapov A 2010 *Phys. Rev. Lett.* **105** 030404
[32] Dyke P, Kuhnle E D, Whitlock S, Hu H, Mark M, Hoinka S, Lingham M, Hannaford P and Vale C J 2011 *Phys. Rev. Lett.* **106** 105304
[33] Sommer A T, Cheuk L W, Ku M J H, Bakr W S and Zwierlein M W 2012 *Phys. Rev. Lett.* **108** 045302
[34] Marsiglio F, Pieri P, Perali A, Palestini F and Strinati G C 2015 *Phys. Rev. B* **91** 054509
[35] Klimin S N, Tempere J and Devreese J T 2012 *New J. Phys.* **14** 103044
[36] Martiyanov K, Barmashova T, Makhalov V and Turlapov A 2016 *Phys. Rev. A* **93** 063622
[37] Murthy P A, Boettcher I, Bayha L, Holzmann M, Kedar D, Neidig M, Ries M G, Wenz A N, Zürn G and Jochim S 2015 *Phys. Rev. Lett.* **115** 010401